Unified Treatment of Rarefied and Continuum Fluid Flows

Kun Xu

Mathematics Department, Hong Kong University of Science and Technology, Kowloon, Hong Kong

1 PRINCIPLES OF UNIFIED SCHEME

The partial differential equation (PDE) of fluid dynamics is constructed to model the physical laws in continuous space and time (Landau and Lifshitz, 1959; Chapman and Cowling, 1990). Similarly, a numerical scheme is to construct the corresponding physical laws, but in a discretized space. To build a valid numerical scheme is more difficult than obtaining the PDEs. Besides the intrinsic scale of the physical phenomena to be considered, such as the particle mean free path or the hydrodynamic dissipative layer, there is a numerical scale to be accounted for as well, that is, the cell size and time step. A unified treatment should be able to capture both kinetic and hydrodynamic scale flow behavior as the mesh size changes in different flow regimes.

In a continuous space, the physical laws for the fluid motion, such as mass, momentum, and energy conservations, are represented as PDEs. Even though the space is continuous, the PDEs are valid only in the description of the physical reality in its modeled scale. With the changing of modeling scales, for a gas flow the governing equations can be changed from the Liouville's equation, the Boltzmann equation, up to the Navier–Stokes equations. Traditionally, a numerical scheme is regarded as a direct numerical discretization of the governing equation of the continuous space. For example, the name of numerical partial differential equation is frequently used. This kind of methodology may be problematic, because the intrinsic physical scale of the PDEs may be different from the numerical mesh size scale. In order to laid the numerical computation on a solid foundation, the physical modeling has to be done directly in a discretized space.

A numerical scheme should be a direct representation of the physical laws in a discretized space. The physical laws are the basic mass, momentum, and energy conservations for the gas motion. Therefore, in a control volume of the discretized space, the change of any flow variable, such as the density or the particle distribution function, depends on the fluxes across the cell interface and possible source term. The source term can be the body force, such as gravity, for the macroscopic momentum and energy evolution, or the particle collision term for the redistribution of particles in different particle velocity range. In a discretized space, the direct modeling is a representation of physical reality, which is independent of the size of the control volume. However, different scale of the cell size will notify different transport phenomena. The

direct modeling is basically to figure out the corresponding physical phenomena which can be observed in a mesh size scale, that is, the local flow motion across a cell interface. Certainly, the physical reality to be resolved depends on practical engineering requirement and the mesh size resolution. If the cell size is on the scale of molecule diameter, the individual particle motion across the cell interface can be identified. If the cell size comes to a scale of particle mean free path, then the Boltzmann equation can be used to construct the local gas evolution, and figure out the corresponding fluxes (Bird 1994; Aristov, 2001). Here, we need to clearly distinguish between numerical discretization of the Boltzmann equation, or other numerical PDEs, and the PDE-based modeling at the cell interface. For example, in a conventional numerical PDE approach, if f represents the particle distribution function and u is the particle velocity, a direct discretization will approximate uf_x as

$$uf_x = \begin{cases} u(f_j - f_{j-1})/\Delta x, & u > 0, \\ u(f_{j+1} - f_j)/\Delta x, & u < 0. \end{cases} \tag{1}$$

This is the so-called upwinding approximation according to particle velocity. In order to validate the above discretization, there are two underlying assumptions imposed on it. First, the cell size Δx is on the same scale as the physical spatial variation of f. If Δx is on the scale of hundreds particle mean free path, the above approximate is meaningless. Second, the above discretization means that particle takes free transport across the cell interface. If the mesh size is much larger than the particle mean free path, the use of upwinding here is fundamentally flawed, because the particles will not transport freely across the cell interface in the numerical mesh size scale. Instead, the particles will take intensive collision within a time step. Therefore, the direct numerical discretization of PDE may be problematic. On the contrary, we emphasize the concept of PDE-based modeling. The PDE-based modeling is only to use the solution of the PDE to model the gas evolution around the cell interface. If the cell size is on the scale of hundreds of the particle mean free path, the Boltzmann equation with the inclusion of both particle transport and collision will present a time-dependent gas distribution function, which describes the process of gas evolution to the equilibrium state. If the cell size is on the scale less than the particle mean free path, the Boltzmann equation-based modeling will go to particle free transport solution at the cell interface and the above upwinding discretization gets recovered. If the cell size has a scale between the kinetic one (mean free path) and the hydrodynamic one (due to drafting of equilibrium states), the Boltzmann-based modeling should give a nonequilibrium distribution function, which accounts for the competition between the particle collision and transport.

This is the underlying principle for the development of unified scheme. In a discretized space, the time evolution solution of the PDE will be used for the modeling of the particle transport at the cell interface.

2   HYBRID UNIFIED SCHEMES IN AEROSPACE APPLICATIONS

There are many flow problems where both rarefied and continuum flow regimes can exist. An example is a hypersonic flow around a blunt body, where the shock wave and boundary layer with large spatial gradients settle to the nonequilibrium flow regimes, and other smooth regions may be close to the equilibrium one. The Boltzmann equation describes the flow transport in a kinetic scale, that is, the particle mean free path scale, but it can be used in the continuum flow simulation as well if the accumulating effect of particle collision is taken into account properly. Theoretically, a unified scheme which is valid for both continuum and rarefied flows can be developed if the Boltzmann solution is constructed properly in its modeling. Unfortunately, most numerical approaches for the Boltzmann equation have fundamental weakness due to their operator-splitting treatments of the equation.

The Boltzmann equation can be written as $f_t + \mathbf{u} \cdot \nabla f = Q(f)$, where f is the distribution function, $\mathbf{u}$ is the particle velocity, and $Q(f)$ is particle collision term. Many nonequilibrium flow solvers, such as the DSMC and direct Boltzmann solvers (Bird 1994; Aristov 2001; Mieussens, 2000), take the following two steps to solve the Boltzmann equation:
(i) relaxation in accordance to the collisional operator of the Boltzmann equation $\partial f / \partial t = Q(f)$,
(ii) free-molecular transport $\partial f / \partial t = -\mathbf{u} \cdot \nabla f$.

Owing to the above operator-splitting treatment, a valid physical process which is consistent with the above numerical discretization is that the cell size and time step used have to be less than the particle mean free path and collision time. This requirement constraints the extension of the DSMC method and direct Boltzmann solvers to the continuum flow regime, where the cell size used may be many orders larger than the local particle mean free path. Fortunately, for the continuum flow, the Navier–Stokes equations are well-defined and validated. In order to design a unified scheme for both continuum and rarefied flow computations, a combination of NS and DSMC or NS and direction Boltzmann solver becomes a natural choice. Since the Boltzmann solver is much more expensive than NS solver, the NS one should be used as large as possible in the computational domain. Two hybrid methods which are used in aerospace industry is the CFD/DSMC and CFD/Boltzmann solver (Schwartzentruber *et al.*, 2008; Kolobov *et al.*, 2007; Burt *et al.* 2011).

For any hybrid scheme, a boundary between different flow regimes has to be clearly defined, and a valid data exchange between different domains needs to be established. The continuum breakdown parameters are usually defined based on the CFD simulation data, where the flow variable gradients or the NS stress can be directly used to set up a threshold between different domains. For the DSMC/CFD hybrid method, another difficulty is about how to overcome the statistical fluctuation in the DSMC simulations. A CFD solver may be sensitive to the noise introduced through the boundary. However, for the direct Boltzmann solver there is no noise generated at the interface. A smooth transition between CFD and Boltzmann solver can be obtained, especially when a gas-kinetic solver is used for the CFD part (Kolobov *et al.*, 2007; Xu, 2001). The weakness of the CFD/Boltzmann approach is that the direct Boltzmann solver is much more expensive than the DSMC method.

3   UNIFIED SCHEME FOR BOTH CONTINUUM AND RAREFIED FLOWS

The unified scheme is a Boltzmann-equation based modeling method for the particle transport across a cell interface (Xu and Huang, 2010). In the particle evolution process around a cell interface, both particle free transport and collision are taken into account. As a result, the distribution function obtained for the flux evaluation depends on the flow regime and the cell resolution. The unified scheme is a multiscale method with the update of both macroscopic conservative flow variables and microscopic gas distribution function. The novelty of the approach is the coupled treatment of particle transport and collision. The gas distribution function constructed at the cell interface can not only recover the hydrodynamic Chapman–Enskog distribution in the continuum flow regime, but also capture the free molecular transport in the highly nonequilibrium flow region. The distribution function takes a time evolution from nonequilibrium to equilibrium one and the rate for the transition depends on the ratio between time step and particle collision time.

The unified scheme is a finite volume method. In the two-dimensional case, the physical space is divided into control volume, that is, $\Omega_{i,j} = \Delta x \Delta y$ with the cell sizes $(\Delta x) = x_{i+1/2,j} - x_{i-1/2,j}$, $\Delta y = y_{i,j+1/2} - y_{i,j-1/2}$ in the rectangular case. The temporal discretization is denoted by t^n for the n_{th} time step. The particle velocity space is discretized by rectangular mesh points with velocity spacing Δu and Δv, and the center of the (k, l)-velocity interval at $(u_k, v_l) = (k\Delta u, l\Delta v)$. The averaged gas distribution function in a physical control volume (i, j), at time step t^n, and around particle

velocity (u_k, v_l), is given by

$$f(x_i, y_j, t^n, u_k, v_l) = f_{i,j,k,l}^n$$
$$= \frac{1}{\Delta x \Delta y \Delta u \Delta v} \int_{\Omega_{i,j}} \int_{\Delta u \Delta v} \int_{-\infty}^{+\infty} f(x, y, t^n, u, v, w)$$
$$\times \, \mathrm{d}x\mathrm{d}y\mathrm{d}u\mathrm{d}v\mathrm{d}w, \tag{2}$$

where w is the particle velocity in the z-direction.

The time evolution of an averaged gas distribution function inside a physical control volume is due to the particle transport through cell interface and the particle collisions inside each cell to redistribute particle in velocity space. The fundamental governing equation in a discretized space is

$$f_{i,j}^{n+1} = f_{i,j}^n + \frac{1}{\Omega_{i,j}} \int_{t^n}^{t^{n+1}} \sum_{m=1}^{m=n} u_m \hat{f}_m(t) \Delta S_m \mathrm{d}t$$

$$+ \frac{1}{\Omega_{i,j}} \int_{t^n}^{t^{n+1}} \int_{\Omega_{i,j}} Q(f)\mathrm{d}\Omega\mathrm{d}t, \tag{3}$$

where $\hat{f}_m$ is the gas distribution function at a cell boundary, n is the total number of piecewise linear interfaces of a control volume $\Omega_{i,j}$, u_m is the particle velocity normal to the cell interface, ΔS_m is the m-th interface length, and $Q(f)$ is the particle collision term. The above scheme is a direct physical modeling in a discretized space, which is the fundamental numerical governing equation, which has the equivalent importance as the PDE in the continuum space and time.

If we take conservative moments ψ_α on Equation (3), that is,

$$\boldsymbol{\psi} = (\psi_1, \psi_2, \psi_3, \psi_4)^\top = (1, u, v, \frac{1}{2}(u^2 + v^2 + w^2))^\top,$$

and $\mathrm{d}\Xi = \mathrm{d}u\mathrm{d}v\mathrm{d}w$ is the volume element in the phase space, due to the conservation of conservative variables during particle collision, the update of conservative variables becomes

$$W_{i,j}^{n+1} = W_{i,j}^n + \frac{1}{\Omega_{i,j}} \int_{t^n}^{t^{n+1}} \sum_{m=1}^{m=n} \Delta \mathbf{S}_m \cdot \mathbf{F}_m(t)\mathrm{d}t, \tag{4}$$

where W is the averaged conservative mass, momentum, and energy densities inside each control volume, and $\mathbf{F}$ is the corresponding flux for the macroscopic flow variables across the cell interface. This flux will be modeled by constructing the solution of the kinetic equation.

The modeling of gas evolution around a cell interface in the unified scheme can be based on the gas-kinetic BGK model

(Bhatnagar *et al.*, 1954), the Shakhov model (Shakhov, 1968), the ES model, or even the full Boltzmann equation (Chapman *et al.*, 1990). For simplification, only the flux evaluation in the *x*-direction will be presented below. The BGK equation in the *x*-direction is

$$f_t + u f_x = \frac{g - f}{\tau}, \tag{5}$$

where f is the gas distribution function, g is the equilibrium state approached by f, and τ is the particle collision time. Both f and g are functions of space x, time t, particle velocities (u, v), and random velocity w in the z-direction. The particle collision time τ is related to the viscosity and heat conduction coefficients. The equilibrium state is a Maxwellian distribution,

$$g = \rho \left(\frac{\lambda}{\pi} \right)^{\frac{3}{2}} e^{-\lambda((u-U)^2 + (v-V)^2 + w^2)},$$

where ρ is the density, U and V are the macroscopic velocities in the *x* and *y* directions, and $\lambda = m/2kT$, where m is the molecular mass, k is the Boltzmann constant, and T is the temperature. Since mass, momentum and energy are conserved during particle collisions, f and g satisfy the conservation constraint,

$$\int (g - f)\psi_\alpha d\Xi = 0, \qquad \alpha = 1, 2, 3, 4, \tag{6}$$

at any point in space and time, and $d\Xi = dudvdw$.

The general solution f of the BGK model (Equation (5)) at a cell interface $x_{j+1/2}$ and time t is,

$$f(x_{j+1/2}, t, u, v, w) = \frac{1}{\tau} \int_0^t g(x', t', u, v, w) e^{-(t-t')/\tau} dt'$$
$$+ e^{-t/\tau} f_0(x_{j+1/2} - ut), \tag{7}$$

where $x' = x_{j+1/2} - u(t - t')$ is the particle trajectory and f_0 is the initial gas distribution function f at the beginning of each time step ($t = 0$). Two unknowns g and f_0 must be specified in Equation (7) in order to obtain the solution f. The above integral solution presents a gas evolution in different physical scales. The f_0 term takes into account the particle free transport in a kinetic scale. The integration of the equilibrium state along the particle trajectory shows the hydrodynamic scale physics, which converges to the Chapman–Enskog expansion in the continuum flow limit. The weights between the kinetic and hydrodynamic flow transport in the determination of final distribution function depend on the ratio of time step to particle collision time. The integral solution plays a key role in the construction of unified scheme for both continuum and rarefied flows.

3.1 Gas-Kinetic Scheme for Continuum Flows

The reason we introduce the gas-kinetic scheme (GKS) for the continuum flow is that the unified gas-kinetic scheme (UGKS) for all flow regimes is a natural extension of GKS. To fully understand GKS will be helpful for easy acceptance of the unified method. For the continuum flow computation, theoretically we only need to update macroscopic flow variables. Therefore, instead of solving Equation (3) for the update of gas distribution function, it is fully legitimate to update the macroscopic flow variables (Equation (4)) only. Even though there is no source term inside each control volume, a time-dependent gas distribution function with the inclusion of particle collision is still needed to evaluate the interface fluxes. This distribution function should converge to the Chapman–Enskog distribution if the flow structure is well resolved in the continuum regime. For the GKS developed progressively in the past years (Xu, 2001), the integral solution of the kinetic Equation (7) is used for the construction of interface f. For the continuum flow simulation, the initial gas distribution function f_0 in Equation (7) is reconstructed using the Chapman–Enskog expansion. The real numerical challenge for the continuum flow computation is about how to handle the discontinuous solution, such as shocks, because in the continuum flow regime we cannot use a mesh size to fully resolve the highly nonequilibrium dissipative shock layer. Therefore, the corresponding kinetic scheme here should be a shock capturing method.

The GKS is for the NS solutions. Based on the macroscopic flow variables around a cell interface, the initial gas distribution function f_0 is constructed from the Chapman–Enskog expansion of the BGK model,

$$f_0 = \begin{cases} g^l \left[1 + a^l x - \tau(a^l u + A^l) \right], & x \leq 0 \\ g^r \left[1 + a^r x - \tau(a^r u + A^r) \right], & x \geq 0 \end{cases}, \tag{8}$$

where the terms being proportional to τ are the nonequilibrium NS states. The parameters of (a^l, A^l, a^r, A^r) are related to the Taylor expansion of a Maxwellian, such as $a^l = (\partial g^l / \partial x)/g^l$ and $A^l = (\partial g^l / \partial t)/g^l$. The nonequilibrium parts have no direct contribution to the conservative variables, that is,

$$\int (a^l u + A^l) \psi g^l d\Xi = 0,$$
$$\int (a^r u + A^r) \psi g^r d\Xi = 0, \tag{9}$$

which are used to evaluate A^l and A^r. The equilibrium state g around $(x = 0, t = 0)$ is modeled to have two slopes,

$$g = g_0 \left[1 + (1 - H[x])\bar{a}^l x + H[x]\bar{a}^r x + \bar{A}t \right], \tag{10}$$

where H[x] is the Heaviside function defined as

$$H[x] = \begin{cases} 0, & x < 0, \\ 1. & x \geq 0. \end{cases}$$

Here g_0 is a local Maxwellian distribution function located at $x = 0$. Even though, g is continuous at $x = 0$, but it has different slopes at $x < 0$ and $x > 0$.

After determining all parameters in the initial gas distribution function f_0 and the equilibrium state g, and substituting Equations (8) and (10) into Equation (7), the gas distribution function f at a cell interface can be expressed as

$$
\begin{aligned}
f(x_{j+1/2}, t, u, v, w) = {} & (1 - e^{-t/\tau})g_0 \\
& + \left(\tau(-1 + e^{-t/\tau}) + te^{-t/\tau}\right)\left(\bar{a}^l H[u]\right. \\
& + \bar{a}^r (1 - H[u])\left.\right) u g_0 \\
& + \tau(t/\tau - 1 + e^{-t/\tau})\bar{A}g_0 \\
& + e^{-t/\tau}\left((1 - u(t + \tau)a^l)H[u]g^l\right. \\
& + (1 - u(t + \tau)a^r)(1 - H[u])g^r\left.\right) \\
& + e^{-t/\tau}\left(-\tau A^l H[u]g^l - \tau A^r (1 - H[u])g^r\right).
\end{aligned}
\tag{11}
$$

Then, the time-dependent numerical fluxes in the x-direction across the cell interface can be computed using the above distribution function

$$F_{j+1/2,\alpha} = \int u \psi_\alpha f(x_{j+1/2}, t, u, v, w)\mathrm{d}\Xi.$$

By integrating the above equation to the whole time step, we can get the total mass, momentum, and energy transport. Starting from a discontinuity, instead of solving the Riemann problem, the gas evolution in the GKS depends on the ratio of time step to the particle collision time. Equation (11) describes such a relaxation process from the free molecule transport to the equilibrium state development. In terms of the CFD methodology, the above gas distribution function is actually a unification of central difference and upwinding schemes. The gas evolution process is a passage from the initial upwinding (free molecule transport or flux vector splitting) to the central differencing (the integration over a continuous equilibrium state). The GKS is a kinetic equation-based modeling method. The nonsmoothness of the initial data f_0, and the equilibrium state construction, are models for the evaluation of a local solution. The kinetic equation is used only for modeling a local solution. So, it should not be surprising that the Prandtl number in the GKS can be fixed easily to a correct value (Xu, 2001). The GKS

has been tested and validated extensively in the past years (Xu *et al.*, 2005; Li *et al.*, 2011).

3.2 Unified Gas-Kinetic Scheme for All Flow Regimes

For rarefied flow computation, besides the updating of macroscopic flow variables, we have to update the gas distribution function as well. The main distinguishable feature of the unified gas-kinetic scheme (UGKS) from the above GKS is that the initial gas distribution function f_0 is known, which can be directly used in the integral solution (Equation (7)). The unified scheme will update both macroscopic flow variables (Equation (4)) and microscopic gas distribution function (Equation (3)).

Same as the GKS, at the cell interface the solution $\hat{f}_{j+1/2,k,l}$ in UGKS is constructed from the integral solution (Equation (7)). Since the gas distribution function is known in the unified scheme, the initial gas distribution function can be constructed directly,

$$
\begin{aligned}
f_0(x, t^n, u_k, v_l, w) & = f_{0,k,l}(x, 0) \\
& = \begin{cases} f^L_{j+1/2,k,l} + \sigma_{j,k,l}x, & x \leq 0, \\ f^R_{j+1/2,k,l} + \sigma_{j+1,k,l}x, & x > 0, \end{cases}
\end{aligned}
\tag{12}
$$

where nonlinear limiter is used to reconstruct $f^L_{j+1/2,k,l}$, $f^R_{j+1/2,k,l}$ and the corresponding slopes $\sigma_{j,k,l}$, $\sigma_{j+1,k,l}$. For the integral part of the equilibrium state in Equation (7), the same distribution as the GKS, that is, Equation (10), is used. The gas distribution function $\hat{f}(x_{j+1/2}, t, u_k, v_l, w)$ at the discretized particle velocity (u_k, v_l) can be expressed as

$$
\begin{aligned}
\hat{f}_{j+1/2,k,l}&(x_{j+1/2}, t, u_k, v_l, w) \\
= {} & (1 - e^{-t/\tau})g_0 \\
& + \left(\tau(-1 + e^{-t/\tau}) + te^{-t/\tau}\right) \\
& \quad \left(\bar{a}^l H[u_k] + \bar{a}^r (1 - H[u_k])\right) u_k g_0 \\
& + \tau(t/\tau - 1 + e^{-t/\tau})\bar{A}g_0 \\
& + e^{-t/\tau}\left((f^L_{j+1/2,k,l} - u_k t \sigma_{j,k,l})H[u_k]\right. \\
& + (f^R_{j+1/2,k,l} - u_k t \sigma_{j+1,k,l})(1 - H[u_k])\left.\right) \\
\triangleq {} & \tilde{g}_{j+1/2,k,l} + \tilde{f}_{j+1/2,k,l},
\end{aligned}
\tag{13}
$$

where $\tilde{g}_{j+1/2,k,l}$ is all terms related to the integration of the equilibrium state g, and $\tilde{f}_{j+1/2,k,l}$ is the terms from initial condition f_0.

In the continuum flow region, due to the sufficient number of particle collisions and with the condition of time step being much larger than the local particle collision time, the contribution from the integration of the equilibrium state $\tilde{g}_{j+1/2,k,l}$ will be dominant in the final solution of the distribution function $\hat{f}_{j+1/2,k,l}$. The $\tilde{g}_{j+1/2,k,l}$ itself gives a corresponding NS distribution function, and the contribution from initial term $\tilde{f}_{j+1/2,k,l}$ vanishes. In the highly nonequilibrium region, such as inside the dissipative shock layer, where the cell size is less than the particle mean free path, the nonequilibrium part $\tilde{f}_{j+1/2,k,l}$ will make a dominant contribution.

In order to discretize the collision term in Equation (3) efficiently, the UGKS will update the macroscopic variables first, see Equation (4), using the the gas distribution function (Equation (13)) for the flux evaluation. Then, the updated macroscopic flow variables will be used to treat the collision term in Equation (3) implicitly. In general, based on the updated conservative variables (Equation (4)), we can immediately obtain the equilibrium state $g_{i,j,k,l}^{n+1}$ inside each cell, therefore based on Equation (3) and kinetic BGK collision model, the UGKS updates the gas distribution function as

$$
\begin{aligned}
f_{i,j,k,l}^{n+1} = \left(1 + \frac{\Delta t}{2\tau^{n+1}}\right)^{-1} & \left[f_{i,j,k,l}^{n} + \frac{1}{\Omega_{i,j}} \int_{t^n}^{t^{n+1}} \right. \\
& \sum_m \Delta S_m u_m \hat{f}_{m,k,l} \mathrm{d}t \\
& \left. + \frac{\Delta t}{2} \left(\frac{g_{i,j,k,l}^{(n+1)}}{\tau_{i,j}^{n+1}} + \frac{g_{i,j,k,l}^{(n)} - f_{i,j,k,l}^{n}}{\tau_{i,j}^{n}} \right) \right], \quad (14)
\end{aligned}
$$

where no iteration is needed for f^{n+1}. The particle collision times $\tau_{i,j}^{n}$ and $\tau_{i,j}^{n+1}$ are defined based on the temperature and pressure of local macroscopic flow variables, that is, $\tau_{i,j}^{n} = \mu(T_{i,j}^{n})/p_{i,j}^{n}$ and $\tau_{i,j}^{n+1} = \mu(T_{i,j}^{n+1})/p_{i,j}^{n+1}$. For the UGKS, due to its implicit treatment of the particle collision term, the time step is not limited by the particle collision time. In the continuum flow regime, we do not intend to resolve the physics in the particle mean free path scale, therefore the unified scheme can take a large time step determined by the CFL condition. Also, the Shakhov model can be used in the above unified framework for modifying the Prandtl number of the scheme (Xu and Huang, 2011).

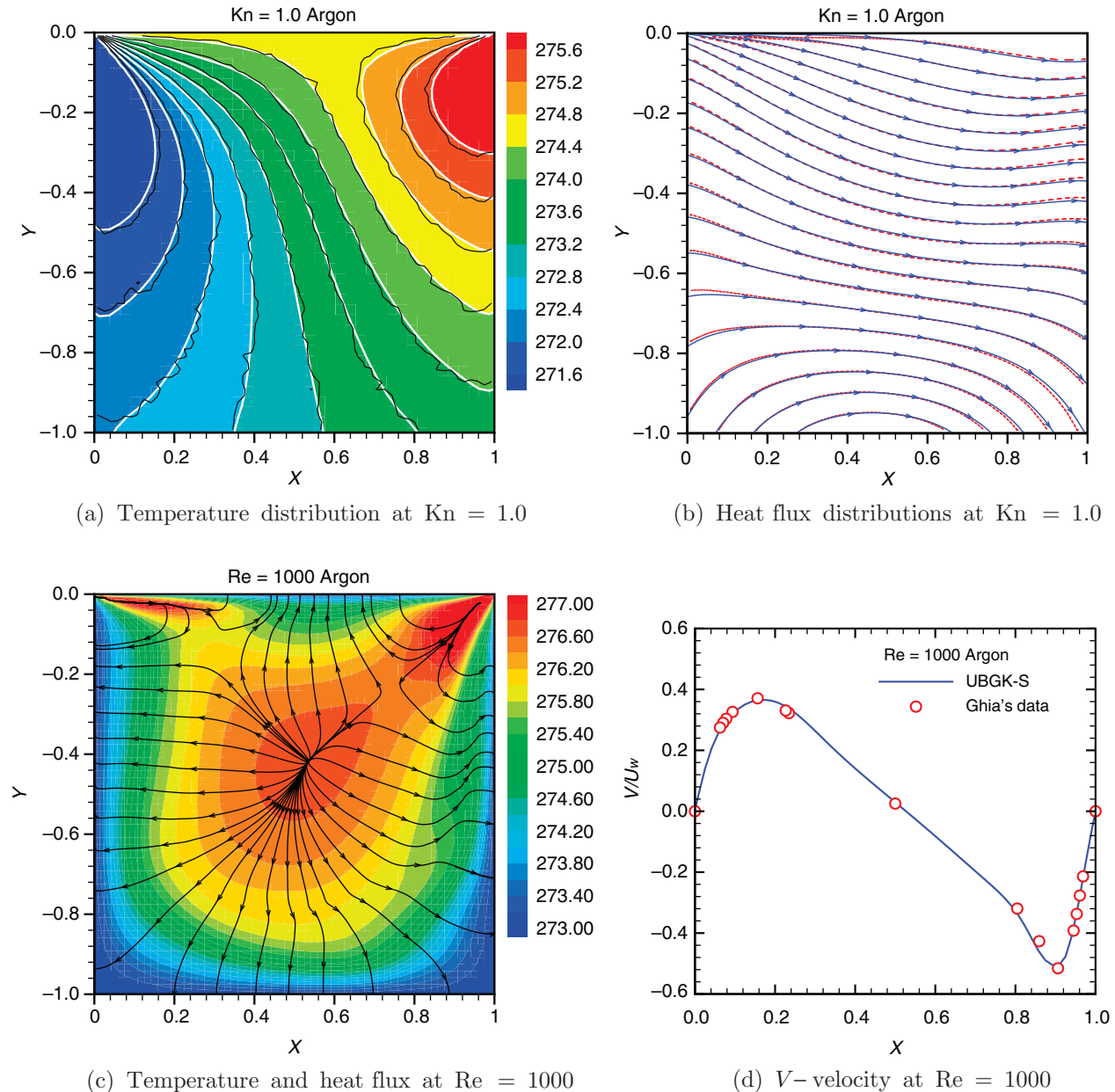## 4 EXAMPLES IN RAREFIED AND CONTINUUM FLOW REGIMES

For nonequilibrium flows, there are limited analytic solutions or experimental measurements. For the circular cylinder case,
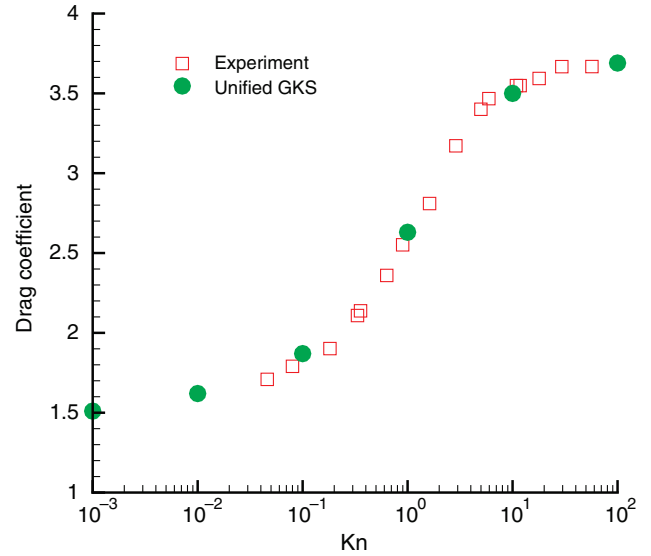
Figure 1. Total drag forces on a circular cylinder at $M = 1.96$ and different Knudsen numbers from 0.001 to 100. Square: experimental data (Maslach and Schaaf, 1963) and solid circles: UGKS solution.

the experimental measurements for the drag coefficients at different Mach and Knudsen numbers are available (Maslach and Schaaf, 1963). To illustrate the capability of the UGKS for the whole flow regime simulation, we calculate the circular cylinder case at Mach number 1.96 and different Knudsen numbers from 0.001 to 100. Figure 1 presents the comparison between the calculated cylinder drag coefficients and experimental data at different Knudsen numbers. It is shown that the computed results agree with the experimental data very well.

The second case is the cavity flow presented by John *et al.*, (2011), which is about the study of nonequilibrium heat transfer using parallel DSMC method at different Knudsen numbers. The DSMC solution is obtained with 1024 processors on a Blue Gene/P (BGP) supercomputer. For all flow calculations, the gaseous medium is assumed to consist of monatomic molecules corresponding to that of argon with mass, $m = 6.63 \times 10^{-26}$ kg. In the DSMC solution, the variable hard sphere (VHS) collision model has been used, with a reference particle diameter of $d = 4.17 \times 10^{-10}$ m. The wall temperature is kept the same as the reference temperature, that is, $T_\mathrm{w} = T_0 = 273$ K. In the current study, the wall velocity is fixed, that is, $U_\mathrm{w} = 50$ m/s. The Knudsen number variation is achieved by varying the density. Maxwell model is used to represent surface accommodation, where in the current study only the case with full wall accommodation is presented. Figure 2a and b shows the comparison between DSMC and the UGKS solution at Kn = 1.0 (Huang, *et al.*, 2011), where the heat flux is going from cold to hot region.

(a) Temperature distribution at Kn = 1.0

(b) Heat flux distributions at Kn = 1.0

(c) Temperature and heat flux at Re = 1000

(d) V−velocity at Re = 1000

Figure 2. Cavity simulation using unified scheme at Kn = 1.0 (a,b), and Re = 1000 (c,d). (a) Black line: DSMC, white line: UGKS, (b) black line: DSMC, red-dash line: UGKS, (c) temperature contours and heat flux by UGKS, (d) V-velocity along central horizontal line, circles: NS solution, line: UGKS.

Since the UGKS can be used for continuum flow computation as well, the simulation at Reynolds number Re = 1000 for the cavity case is presented in Figures 2c and d, where the solution is compared with the benchmark NS solution in continuum flow regime. For the continuum flow at Re = 1000, the heat flux does satisfy the Fourier's law, which is from hot to cold region. The UGKS basically recovers the GKS solution in the continuum regime for the NS solution.

In the low speed transition flow regime, there are many interesting phenomena related to heat transfer. Thermal creep flow is induced in a channel or a pipe because the temperature gradient along the wall boundary (Karniadakis *et al.*, 2005). The induced flow will be in the direction of the temperature gradient. This phenomenon is usually explained according to "slip" gas/solid boundary condition in the presence of appreciable temperature gradients along the interface. The
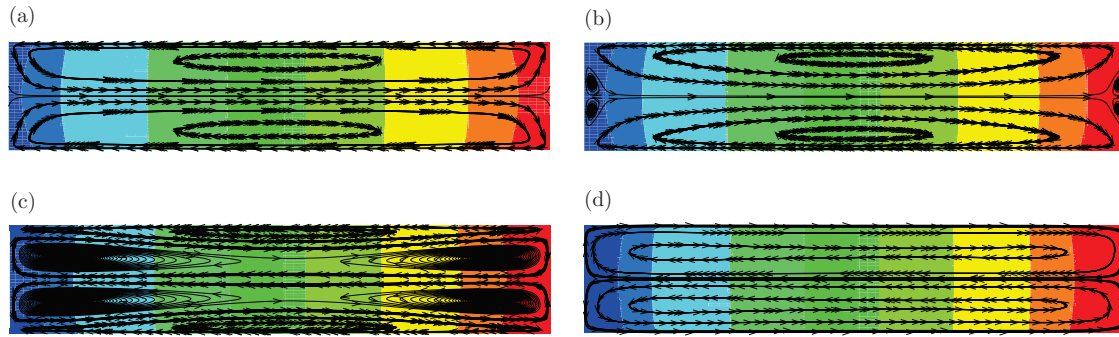
Figure 3. Thermal creep instability for a closed tube with length to width ratio $L/D = 5$, and 10 k temperature differences from the left to right ends along the tube surfaces. The particle mean free path for the argon gas inside the tube is 64 nm. (a) $D = 50$ nm. (b) $D = 100$ nm. (c) $D = 200$ nm. (d) $D = 400$ nm.

commonly accepted theory claims that the flow close to the boundary will move from the cold to hot region, then return in the middle for a closed tube. The UGKS simulation shows that the flow patterns depend on the temperature gradients and Knudsen numbers, which are much more complicated than people originally think of. Figure 3 shows the simulation results for a closed tube with aspect length/width ratio 5, 10 k temperature difference from left to right ends, and different tube widths of 50, 100, 200 and 400 nm. The argon gas inside tube has a mean free path of 64 nm. Surprisingly, with the change of Knudsen numbers or tube width, the flow can move along the tube surface from the hot to cold regions. This observation contradicts with the current

theoretical prediction. Also, between the simple clockwise and anticlockwise vortex rotations, such as the cases with 50 nm and 400 nm tube widths, there are complicated transition flow patterns between them with a variation of tube width. The analysis of the above flow pattern is more difficult than the analysis for the Rayleigh Bernard instability, because here there are no well-defined macroscopic governing equations. We would like to call the above anomalous phenomena in the transition flow regime as thermal creep instability, where the flow patterns will depend on Knudsen numbers, temperature gradients, and aspect ratios of the tube.

The direct simulation Monte Carlo (DSMC) method has been validated extensively through the shock structure
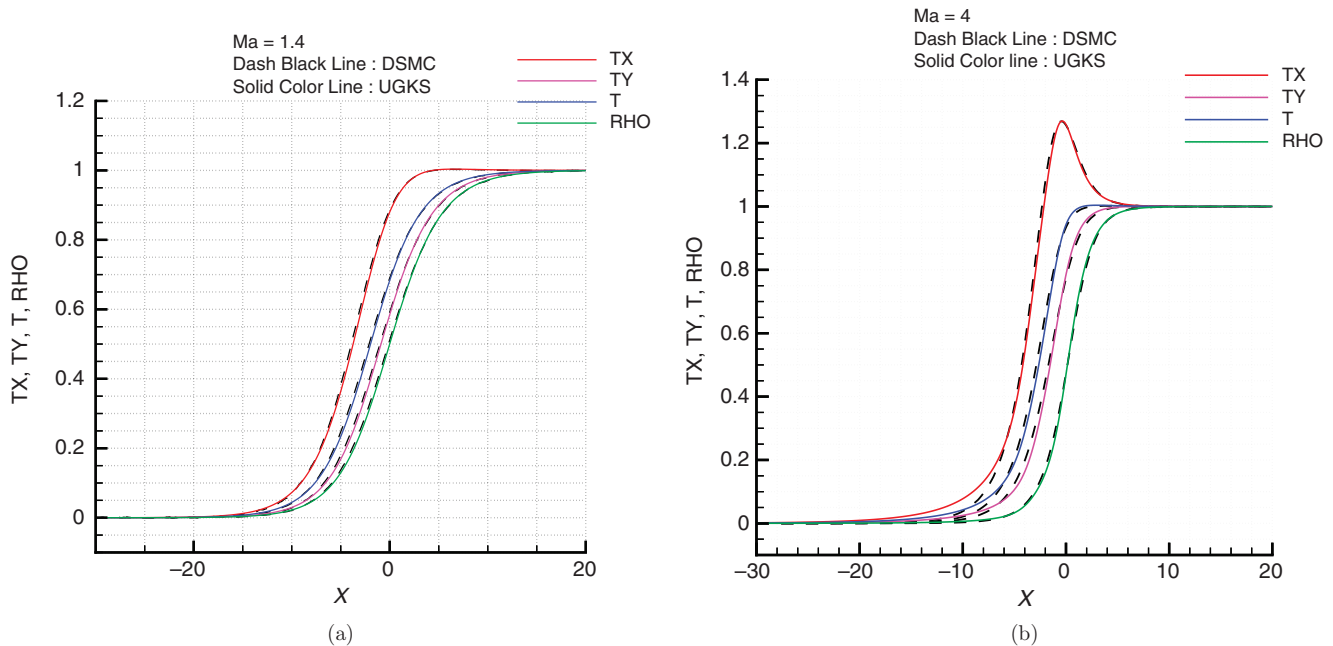
Figure 4. DSMC and UGKS solutions for the argon shock structures at $M = 1.4$ and 4. (a) Density and temperatures at $M = 1.4$. (b) Density and temperatures at $M = 4$.

(a) Sound speed vs frequency

(b) Absorption coefficients vs frequency
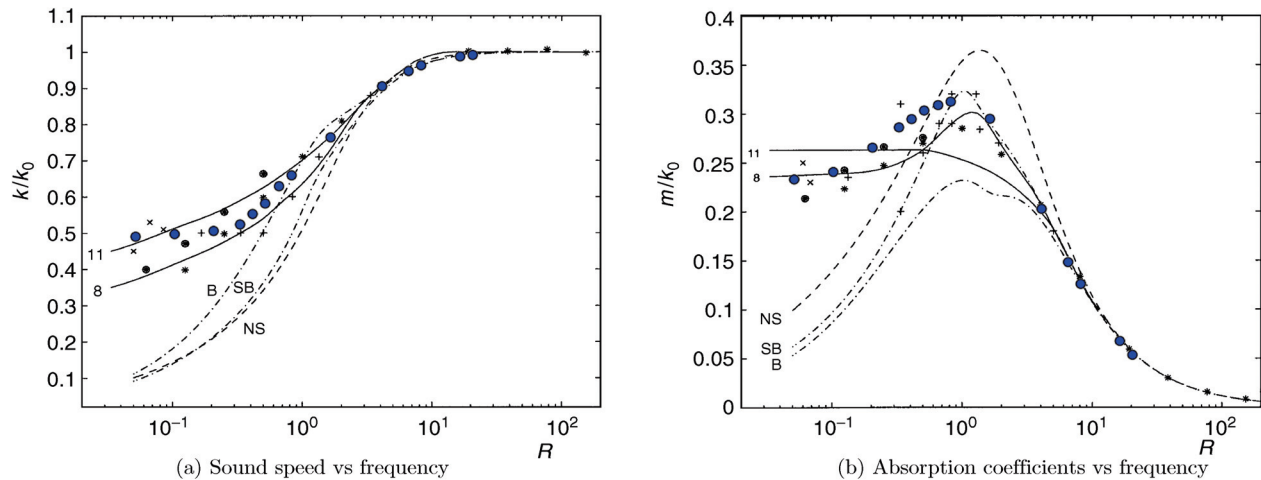
Figure 5. (a) Scaled inverse sound speed vs scaled inverse frequency. The solid lines represent the 8 and 11 moment solutions, the dashed line represents the Navier–Stokes prediction, the dash-dotted lines represent the Burnett and super-Burnett solutions, the crosses represent experimental data, and the closed stars and plain stars are the DSMC simulation results (Hadjiconstantinou and Garcia, 2001), and the solid blue circles are UGKS solutions. (b) Scaled absorption coefficient vs scaled inverse frequency. The solid lines represent the 8 and 11 moment solutions, the dashed line represents the Navier–Stokes prediction, the dash-dotted lines represent the Burnett and super-Burnett solutions, the crosses represent experimental data, the stars closed star and plain stars are the DSMC simulation results, and the solid blue circles are UGKS solutions.

calculations in the past decades (Bird, 1994). For the argon gas, we compare the shock structure calculations at Mach number 1.4 and 4 using both DSMC and unified scheme in Figure 4, where the density and directional temperatures are plotted.

The simulations of sound waves propagating in a dilute hard sphere gas have been performed using the unified scheme (Wang *et al.*, 2012). A wide range of frequencies is investigated, including very high frequencies for which the period is much shorter than the mean collision time. In Figure 5, the simulation results are compared to experimental data and approximate solutions of the Boltzmann equation, and the DSMC solution (Hadjiconstantinou and Garcia, 2001). The unified results cover a wide range of wave frequency and give the best results in comparison with experiment measurements among all numerical and analytical solutions.

5   CONCLUDING REMARKS

The UGKS provides a general framework for the construction of unified scheme for all Knudsen number flow computations. The use of the BGK-type particle collision model is only one of the choices. Any realistic kinetic model, even the Boltzmann equation itself, with both particle transport and collision can be used for the flux modeling at the cell interface. The important ingredient in the UGKS is that the physical phenomena observed in a discretized space depend

on the cell resolution. The integral solution used in the construction of local distribution function provides a passage from the kinetic to hydrodynamic scale gas evolution. Which flow physics the numerical scheme can represent depends on the ratios of cell size over the particle mean free path, or the time step over the particle collision time. Since the UGKS updates both macroscopic and microscopic flow variables with a time accurate evolution, the UGKS can be regarded as a multiscale and multiresolution method. The UGKS has been validated in the transition flow regime through enormous amount of test cases. It is optimistic that the UGKS will play an important role in the study of nonequilibrium flows.

REFERENCES

Aristov, V.V. (2001) *Direct Methods for Solving the Boltzmann Equation and Study of Nonequilibrium Flows*, Kluwer Academic Publishers.

Bhatnagar, P.L., Gross, E.P. and Krook M. (1954) A model for collision processes in gases I: small amplitude processes in charged

and neutral one-component systems, *Physical Review*, **94**, 511–525.

Bird, G.A. (1994) *Molecular Gas Dynamics and the Direct Simulation of Gas Flows*, Oxford Science Publications.

Burt, J.M., Josyula, E., Deschenes, T.R. and Boyd, I.D. (2011) Evaluation of a hybrid boltzmann-continuum method for high-speed nonequilibrium flows, *Journal of Thermophysics and Heat Transfer* **25**, 500–515.

Chapman, S. and Cowling, T.G. (1990) *The Mathematical Theory of Non-uniform Gases*, Cambridge University Press.

Hadjiconstantinou, N.G. and Garcia, A.L. (2001) Molecular simulations of sound wave propagation in simple gases, *Physics of Fluids*, **13**, No. 4, 1040–1046.

Huang, J.C., Xu, K. and Yu, P.B. (2011) A unified gas-kinetic scheme for continuum and rarefied flows II: multi-dimensional cases, *Communications in Computational Physics*, **3**(2012), No. 3, 662–690.

John, B., Gu, X.J. and Emerson, D.R. (2011) Effects of incomplete surface accommodation on non-equilibrium heat transfer in cavity flow: a parallel DSMC study, *Computer and Fluids*, **45**, 197–201.

Karniadakis,G., Beskok, A. and Aluru, N. (2005) *Microflows and Nanoflows*, Springer Verlag.

Kolobov, V.I., Arslanbekov, R.R., Aristov, V.V., Frolova, A.A. and Zabelok, S.A. (2007) Unified solver for rarefied and continuum flows with adaptive mesh and algorithm refinement. *Journal of Computational Physics*, **223**, 589–608.

Landau, L.D. and E.M. Lifshitz (1959) *Fluid Mechanics*, Pergamon Press, London.

Li, J.Q., Li, Q.B. and Xu, K. (2011) Comparison of the generalized Riemann solver and the gas-kinetic scheme for inviscid compressible flow simulations. *Journal of Computational Physics*, **230**, 5080–5099.

Maslach, G.J. and Schaaf, S.A. (1963) Cylinder drag in the transition from continuum to free-molecule flow. *Physics of Fluids* **16**, pp. 315.

Mieussens, L. (2000) Discrete-velocity models and numerical schemes for the boltzmann-BGK equtaion in plane and axisymmetric geometries. *Journal of Computational Physics*, **162**, 429–466.

Schwartzentruber, T.E., Scalabrin, L.C. and Boyd, I.D. (2008) Multiscale particle-continuum simulations of hypersonic flow over a planetary probe. *Journal of Spacecraft Rockets*, **45**, 1196–1206.

Shakhov, E.M. (1968) Generalization of the Krook kinetic equation. *Fluid Dynamics* **3**, pp. 95.

Wang, R.J. and Xu, K. (2012) The study of sound wave propagation in rarefied gases using unified gas-kinetic scheme. *Acta Mechanica Sinica* **28**, 1022–1029.

Xu, K. (2001) A gas-kinetic BGK scheme for the Navier-Stokes equations and its connection with artificial dissipation and Godunov method. *Journal of Computational Physics* **171**, 289–335.

Xu, K. and Huang, J.C. (2010) A unified gas-kinetic scheme for continuum and rarefied flows. *Journal of Computational Physics*, **229**, 7747–7764.

Xu, K. and Huang, J.C. (2011), An improved unified gas-kinetic scheme and the study of shock structures. *IMA Journal of Applied Mathematics*, **76**, 698–711.

Xu, K., Mao, M.L. and Tang, L. (2005) A multidimensional gas-kinetic BGK scheme for hypersonic viscous flow. *Journal of Computational Physics*, **203**, 405–421.